

YALE PEABODY MUSEUM

P.O. BOX 208118 | NEW HAVEN CT 06520-8118 USA | PEABODY.YALE. EDU

JOURNAL OF MARINE RESEARCH

The *Journal of Marine Research*, one of the oldest journals in American marine science, published important peer-reviewed original research on a broad array of topics in physical, biological, and chemical oceanography vital to the academic oceanographic community in the long and rich tradition of the Sears Foundation for Marine Research at Yale University.

An archive of all issues from 1937 to 2021 (Volume 1–79) are available through EliScholar, a digital platform for scholarly publishing provided by Yale University Library at <https://elischolar.library.yale.edu/>.

Requests for permission to clear rights for use of this content should be directed to the authors, their estates, or other representatives. The *Journal of Marine Research* has no contact information beyond the affiliations listed in the published articles. We ask that you provide attribution to the *Journal of Marine Research*.

Yale University provides access to these materials for educational and research purposes only. Copyright or other proprietary rights to content contained in this document may be held by individuals or entities other than, or in addition to, Yale University. You are solely responsible for determining the ownership of the copyright, and for obtaining permission for your intended use. Yale University makes no warranty that your distribution, reproduction, or other use of these materials will not infringe the rights of third parties.



This work is licensed under a Creative Commons Attribution-NonCommercial-ShareAlike 4.0 International License.
<https://creativecommons.org/licenses/by-nc-sa/4.0/>



Phytoplankton growth at the shelf-break front in the Middle Atlantic Bight

by John Marra,¹ R. W. Houghton¹ and Christopher Garside²

ABSTRACT

The summertime front near the shelf break in the Middle Atlantic Bight is both thermohaline and baroclinic. Near the surface, large gradients of temperature (T) and salinity (S) exist with little cross-frontal variation in density. At depths >50 m, an isopycnal boundary separates Slope Water from colder, fresher shelf water. Higher concentrations of chlorophyll are found in the upper part of the front, between water types of shelf and Slope Water origin. Calculations show also that the front is a region of enhanced phytoplankton growth. It is proposed that the relative fertility of the front is the result of large-scale deformations of the T/S boundary between shelf and Slope Water. The entrainment of deep shelf water along the shallowing, seaward-sloping, isopycnals in the deeper part of the front by these large-scale perturbations bring turbid, nutrient-rich water into clearer water that is also nutrient poor. The combination of this nutrient enrichment and a well-lighted water column makes the front more productive than elsewhere.

1. Introduction

As in the atmosphere, ocean fronts are regions of strong dynamic interactions. Ocean fronts are classified into two types: density (or baroclinic) fronts and thermohaline fronts. Baroclinic fronts have sharp lateral density gradients, while in the latter there are large, but density-compensating gradients of temperature and salinity, where colder, fresher water borders water that is warmer and saltier. Thermohaline fronts have been less well-studied than the baroclinic kind. The maintenance of frontal systems in counteraction to dispersive mixing, and the reasons for the oft-reported high biological activity (e.g. Pingree *et al.*, 1975; Fournier *et al.*, 1977; Kinder *et al.*, 1983; Holligan and Groom, 1986) remain issues to be resolved.

The frontal system that occurs at the shelf-break in the Middle Atlantic Bight, exhibits features of both a density front and a thermohaline front. A baroclinic front occurs in late winter and spring and extends from the surface to the bottom. A region of enhanced phytoplankton biomass (as indicated by chlorophyll a) is found near the surface, just shoreward of the front. The inclination of the isopycnals which mark the

1. Lamont-Doherty Geological Observatory of Columbia University, Palisades, New York, 10964, U.S.A.

2. Bigelow Laboratory for Ocean Sciences, West Boothbay Harbor, Maine, 04575, U.S.A.

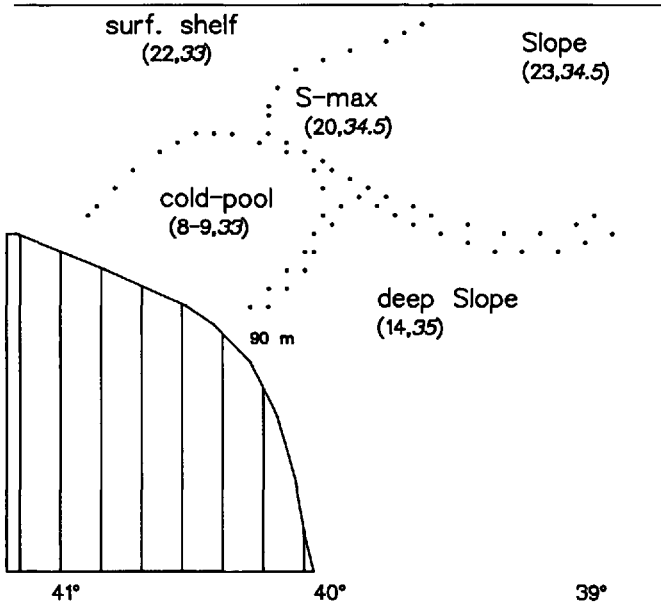


Figure 1. Schematic of the water masses bordering the shelf-break front. The numbers in parentheses for each water mass indicate typical values for summertime temperature and salinity (T, S). Approximate latitudes (N) are given across the bottom, and the depth (90 m) where the cold pool intersects the bottom. The transects on this cruise were from approximately $40^{\circ}20' N$ to $39^{\circ} N$.

front stabilizes the water column there, creating a region favorable for phytoplankton growth (Marra *et al.*, 1982).

In late spring and summer, the near-surface front becomes thermohaline as surface heating of coastal water produces shelf and Slope Water with the same thermal characteristics, and large salinity gradients develop along isopycnal surfaces. The baroclinic boundary, inclining seaward from the shelf-break, is still present but only at depths $>40\text{--}50$ m (Fig. 1). Above this, and at the base of the seasonal pycnocline, Slope Water sometimes intrudes, causing a mid-depth salinity maximum, the *S-max* (Gordon and Aikman, 1981). Deeper shelf water, the cold-pool, underlies the warm surface water and the *S-max*. The cold-pool is so named because it retains its wintertime temperature (Houghton, *et al.*, 1982). Deep Slope Water (found deeper than $40\text{--}50$ m) and seaward of the shelf break is identified by being warmer and more saline than the cold pool. Thus we can identify up to five different water-types at the front: (1) coastal surface water, (2) surface Slope Water, (3) the *S-max* intrusion, (4) cold pool water, (5) and deep Slope Water (Fig. 1).

The biological structure and dynamics associated with the summertime thermohaline fronts are more difficult to explain than the baroclinic type, since unlike the spring, nutrient distributions assume greater importance, and maintenance of the front

may be achieved through subtle physical processes (Houghton and Marra, 1983; hereafter, HM83). The chlorophyll distribution at the thermohaline front in the Middle Atlantic Bight is characterized in the vertical by a subsurface maximum at 20–50 m depth. In the horizontal direction, and normal to the front, the subsurface chlorophyll structure exhibits a variability relative to the thermohaline boundary.

The data from HM83 for biological determinants of the chlorophyll distributions suffered from lack of high-resolution data for nutrients and light. Also, we did not have enough data either seaward or shoreward of the front to evaluate the distributions we saw in terms of the larger context of shelf and slope circulation. In summer of 1983, we returned to the thermohaline front over the New England Shelf with the objective of gaining more complete coverage of the nutrient, light and chlorophyll fields. Our goal was to understand the causes of the biological and nutrient distributions near the front, and also to determine what these dynamics can reveal about the physical processes that maintain it. Here we present the results from this field program and offer a mechanism for production of the enhanced phytoplankton biomass observed at the front. Houghton *et al.* (1986), using satellite imagery and shipboard data, illustrate the alongshore variability and three-dimensional structure of the circulation and these are essential to interpret the cross-shelf structure at the front.

2. Methods

The cruise (designated SWIG IV) was carried out aboard R/V *Cape Florida* from 17 July–1 August, 1983. The region of the cruise was near the continental shelf-edge off the Eastern Seaboard of the U.S., south of Block Island Sound (Fig. 2). The sampling design included two primary modes along the cruise track (Fig. 2). To sample large scale distributions, we completed three long sections along 71W spanning about 160 km. These began well inshore of the front to the Slope Water. The long sections were done at the beginning, middle, and end of the cruise. Several smaller transects were also made in a tow-yo mode, where the ship proceeded slowly, normal to the front, while the sensors were continually raised and lowered in the water column.

Vertical distributions of temperature and salinity were obtained using a Neil Brown Mark III CTD/O₂ system with a fast response thermistor. The CTD was attached to a 12-position rosette which had a set of 1.7 l Niskin samplers. Details on the operation, calibration of the sensors, and data reduction can be found in HM83. We also employed expendable bathythermographs (XBT's) during the long sections for greater resolution of temperature structure than could be obtained from the CTD/O₂ system alone.

We used a submersible pump and hose system to collect water for the analysis of the vertical distributions of chlorophyll and nutrients. The submersible pump was attached to the CTD frame and it pumped water through the hose to a bubble trap (about 10 l capacity) on the 01 level of the ship ("deck" above the main deck). From there, the water was fed by gravity to the laboratory on the main deck and to a Turner Designs

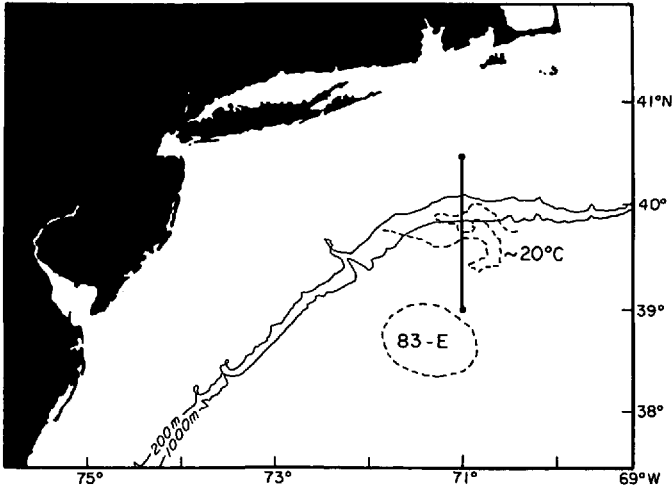


Figure 2. (a) Map of the Middle Atlantic Bight showing the 200 m and 1000 m isobaths. Also shown are an outline of the thermal boundary of the Shelf/Slope front (the 20°C isotherm) and of Ring 83-E derived from a NOAA-7 AVHRR image on 13 July, 1983 (see Houghton *et al.*, 1986). The N-S line at 71°W longitude is the position of the transects spanning the front.

Model 10 fluorometer (with the standard filter set) to record the *in vivo* fluorescence, on a chart recorder (and which also recorded the pressure signal from the CTD). Calibration samples for chlorophyll *a* analysis (Holm-Hansen *et al.*, 1965) were collected at three depths on each cast from the hose output (and accounting for the time lag of 5 s between fluorometer and drain). The fluorescence profiles were digitized to produce chlorophyll *a* profiles with 1 m resolution.

Water for nutrient analyses was supplied by the same hose, and fed to a Continuous Flow Analyzer (CFA), running analyses for ammonia, nitrate, nitrite, phosphate and silicate (methods modified from Whitledge *et al.* (1981)). The CFA sampled the flow every 2 minutes (1 min. wash:1 min. sample) during the upcast of the CTD rosette. The five analog outputs from the multichannel colorimeter and the correlated analog depth signal from the CTD were digitized every five seconds. Mixed standards, deionized water and artificial seawater baselines were run every two hours to calibrate the colorimeter analog output. The digital records of the data were subjected to a peak-reconstruction technique, and baseline correction. Sample concentration was calculated from the ratio of the sample peak to the mean of the standard peaks, multiplied by the standard concentration.

Three scales of resolution will be seen in the sections shown. For temperature, there are CTD casts as well as XBT's. The salinity distribution relies only on CTD casts. There are chlorophyll and nutrient data only for every other CTD cast. We focus on one nutrient, nitrate, although phosphate and silicate behaved similarly.

A 4-pi quantum sensor with built-in pressure sensor, (QSP-200D Biospherical

Instr.), was used to determine underwater light (photosynthesis available radiation, PAR). Light profiles were taken from the stern of the ship, immediately after the CTD casts, with the ship steaming slowly forward so as to avoid a shadow effect from the ship in the profiles. The diffuse attenuation coefficient for irradiance (PAR), k , was calculated from the profiles of underwater light, fitting that data to the equation,

$$E(z) = E(0) \cdot e^{-kz}, \quad (1)$$

where $E(z)$ is the quantum irradiance at depth z , and $E(0)$ the surface value. Thus, k represents an average over the euphotic zone.

Primary production was measured as the assimilation of $^{14}\text{CO}_2$. These measurements took place *in situ*, in bottles (3 light, 1 dark) held in plexiglass holders, and hung at six depths in the euphotic zone on a line suspended beneath a spar buoy. The buoy was deployed before dawn and recovered after dusk. After recovery, the incubated water was filtered through Whatman GF/F filters which were later counted using standard liquid scintillation methods (Horrocks, 1977). For each depth sampled, a water sample was taken for particulate organic carbon (POC) and nitrogen analysis, determined subsequently on a Perkin-Elmer 240D Elemental Analyzer. We plotted POC against chlorophyll a (Chl) values and calculated a regression relationship of $\text{POC} = 133 \cdot (\text{Chl}) + 56$ ($r^2 = 0.66$).

At specified intervals during the pump casts, sample bottles were filled with water, and a few mls of (acidified) Lugol's solution added for preservation. The samples were later examined for species enumeration in the laboratory under an inverted microscope using the Ütermohl technique.

3. Results

a. Large-scale distributions. To summarize the physical and biological distributions over the course of the cruise, in Figure 3, we have plotted the minimum temperature in a CTD cast and the maximum chlorophyll value in the corresponding pump profile as a function of position and time. The minimum temperature is a marker for shelf water (i.e., the cold pool and its offshore extension) and the maximum chlorophyll value is a marker for phytoplankton concentrations relative to the physical field. For these data, as we later show, the maximum chlorophyll value is a good indicator of the quantity of chlorophyll in the euphotic zone. Figure 3 can only be considered a map of the space-time distributions if the alongshore flow is constant. This is not the case, but Figure 3 summarizes the variability observed in the occurrence of shelf water parcels in Slope Water, and their relationship to phytoplankton distributions, over the course of the cruise.

The temperature minima range from 8°C, indicative of the cold pool on the shelf, to 14°C, the seaward edge of cold-pool water mixed with Slope Water. For the purposes of this analysis, we define a frontal zone as the subsurface boundary defined by a minimum temperature in the range 10–14°C, and shown in Figure 3. This is a

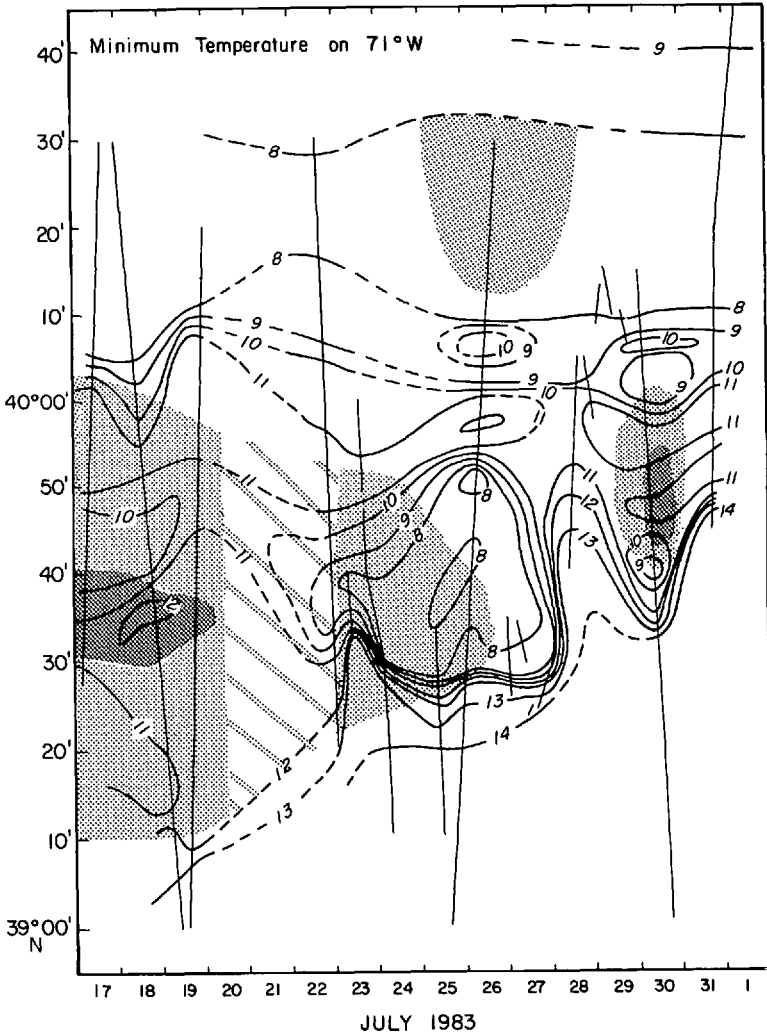


Figure 3. The minimum temperature on each profile (CTD or XBT) plotted as a function of position and time on the cruise. The straight lines represent the positions of transects, with the three long lines spanning the front being the three long sections of the cruise (LS1, LS2, LS3, chronologically). The shorter lines are tow-yo sections as described in the text. Superimposed on this (the shaded areas) is the maximum in chlorophyll for the pump profiles, also as a function of position and time. The minimum temperature marks the position of the cold pool and also indicates the offshore transport of shelf water. Between 20–22 July, the ship returned to port for repair of an engine casualty. Lighter shaded areas correspond to chlorophyll a values $>2 \mu\text{g l}^{-1}$, and darker shaded areas, $>3 \mu\text{g l}^{-1}$. “Background” chlorophyll a values are $1\text{--}2 \mu\text{g l}^{-1}$ shoreward of the 14°C isopleth, and rapidly drop to $<1 \mu\text{g l}^{-1}$ seaward.

high-gradient region (because of parcels of shelf water) between water types that can be identified as either entirely shelf or entirely Slope Water. Geographically, this puts the frontal zone in the region between 40°00'N and 39°25'N, and largely seaward of the 1000 m isobath. (See Fig. 2). Highest chlorophyll *a* concentrations ($\geq 2 \mu\text{g l}^{-1}$) are usually found in this region rather than on either side, but not always. On 25 July we observed comparably high concentrations shoreward of the front.

Houghton *et al.* (1986) summarized the large-scale flow features occurring during the cruise. The most important feature was the appearance (Fig. 2) of an anti-cyclonically turning jet of shelf water moving offshore (Houghton *et al.*, 1986). Thus, much of the structure in Figure 3 and in the sections (see below) is the result of this three-dimensional feature. Combining satellite imagery (AVHRR, Fig. 2) and measured jet velocities we conclude that the shelf water parcel shown in Figure 3 (at 39°40'N, 23–27 July) was removed from the deep shelf within the previous 2 days. By 30 July, the eddy had lost much of its energy (or advected through the area?), and the frontal zone had contracted.

To examine the vertical structure of chlorophyll and nitrate with respect to the front, we show the large-scale transect done at the end of the cruise (Fig. 4). Figure 3 shows this to be a time period after the major impact of the eddy had occurred. Nevertheless, these sections illustrate the large-scale physical, biological and nutrient conditions, and provide clues to the phytoplankton dynamics during this period.

In the physical data (Figs. 4a,b,c) all the water types (shown in Fig. 1) are apparent with the exception of the *S*-max (which is not always observed). The cold pool of shelf water, defined by temperatures less than or equal to 11°C (see HM83), ends abruptly at about 40°00'N (Fig. 4a), and this demarcates the baroclinic front (at depth) in summer (Fig. 4c). The parcels of water of 9–11°C and <34.0 psu south of this suggests the transport of shelf water into the Slope Water region, but along isopycnals, to as far as 39°30'N in this transect. From Figure 2, we regard this as a mixture of shelf and slope waters, but also a part of the three-dimensional structure of the front. That is, the position of the tongue of shelf water crossing 71W in Figure 2 corresponds with the parcels of shelf water seen in Figure 4. The region of cooler-fresher water seaward of the cold pool is a parcel of shelf water mixed to varying degrees with the surrounding Slope Water. Although it appears detached in this section, a satellite image shows that it is connected to the shelf region by the three-dimensional feature. With the exception of streamers of shelf water entrained around impinging warm-core rings, “detached” parcels of shelf water are observed predominantly during the summer (Houghton *et al.*, 1988). Pingree (1978) has pointed out the importance of these eddies to mixing across a front in the English Channel.

The distribution of chlorophyll across the front (Fig. 4d) shows a maximum (or, Chl-max, defined as concentrations of chlorophyll *a* $\geq 1.0 \mu\text{g l}^{-1}$), which is situated near the top of the cold pool tongue and within the nitracline (Fig. 4e). The Chl-max itself reaches a peak ($>2.5 \mu\text{g l}^{-1}$) in the region of the “detached” parcels of shelf

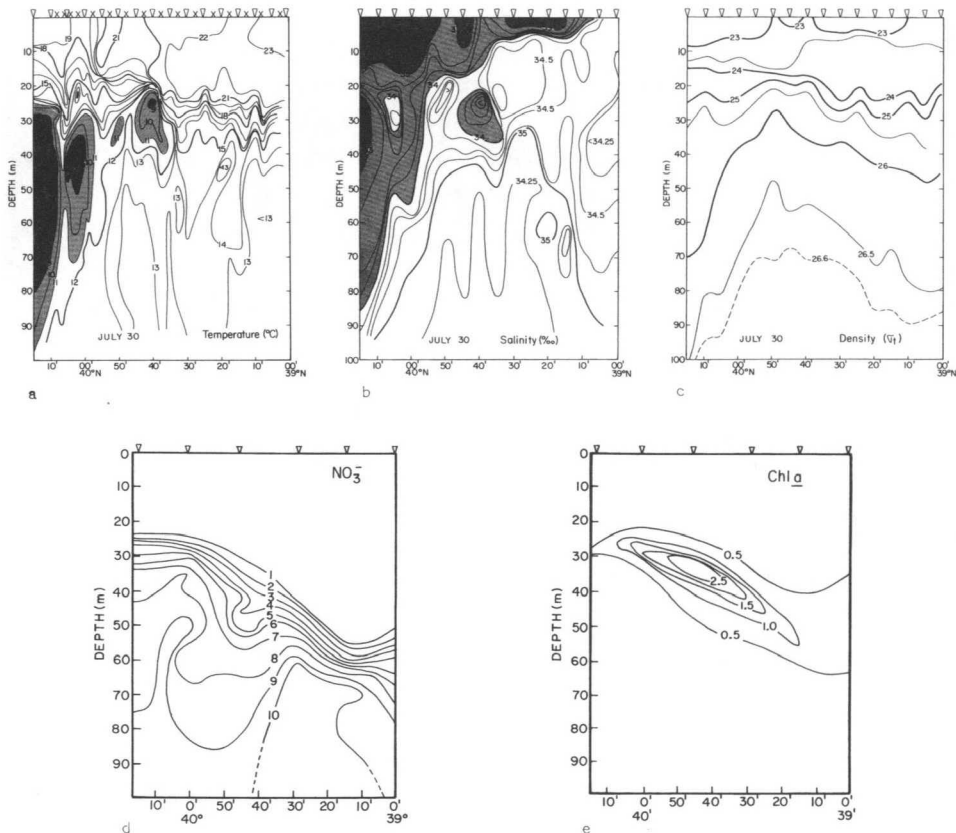


Figure 4. Large-scale transect along 71W completed on July 30, 1983. Inverted triangles across top of panels are positions of CTD (a, b, c) and CTD/pump (d, e) profiles. (a) temperature ($^{\circ}\text{C}$); (b) salinity (psu); (c) σ_t anomaly; (d) NO_3^- ($\mu\text{M l}^{-1}$); (e) chlorophyll *a* ($\mu\text{g l}^{-1}$).

water, and beneath surface Slope Water. Beyond this there is a deepening trend to the Chl-max (and an attenuation of the magnitude) and the nutricline, along the 26.0 σ_t isopycnal. Because both deep Slope Water and cold-pool water have high nitrate, the offshore changes at depth are not dramatic. The cold-pool has typical nitrate values of $6 \mu\text{M l}^{-1}$ and there is an increase to $10 \mu\text{M l}^{-1}$ in deep Slope Water. At 40 m depth, the offshore gradient is from $6 \mu\text{M l}^{-1}$ in the cold pool to $\leq 1 \mu\text{M l}^{-1}$ in Slope Water at the southern end of the transect. Despite the small nitrate gradient across the front, water type properties, and data on the distribution of freons (D. Wallace, personal communication) differentiate the origin of this nutrient on either side of the front.

The diffuse attenuation coefficient for irradiance (PAR) as defined by Eq. (1) declines rapidly going south across the front (Fig. 5) and upon reaching the latitude where the Slope Water (or *S*-max water) appears in the casts, k ceases to decline, staying roughly steady at 0.08 m^{-1} . The corresponding change in euphotic depths (1%

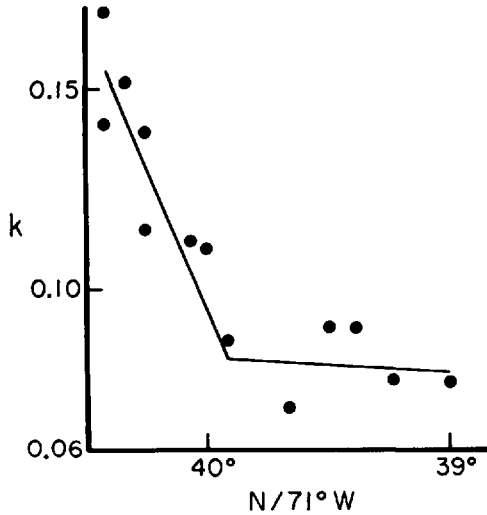


Figure 5. Distribution of the diffuse attenuation coefficient, k (m^{-1}) along 71W. Data is pooled from the entire cruise. The lines are based on a piece-wise fit to a linear regression.

$E(0)$ going offshore is from 35 m over the shelf to 60 m Slope Water. The k data were fit piece-wise using a linear regression of k against geographic position, in each piece omitting the datum at 39°52'N. This approximation to the geographic variation in k is used in the analysis presented below. The abrupt change in the behavior of k at 40N, the latitude where the hydrographic data first indicate the presence of Slope Water, was the breakpoint in the regressions. Since the diffuse attenuation coefficient can distinguish optical water types, it may mark the presence of Slope Water in the surface layers.

b. Phytoplankton distributions and production. All populations that we could distinguish with our methods increase in the frontal region (and are coincident with the increases in chlorophyll), and decline seaward and shoreward (Fig. 6). Diatoms and dinoflagellates are the dominant autotrophs at the Chl-max in the front, and these constitute a common late summer assemblage for the shelf (Malone, 1977). Among the diatoms, *Leptocylindrus danicus*, and *Chaetoceros sp.* are numerically dominant, followed by *Rhizosolenia faeroenese*. *L. danicus* and *R. faeroenese* are common summer diatoms from the inner shelf (Malone, 1977), thus their appearance at the front may indicate transport of shelf water offshore. *Prorocentrum micans* is the most abundant dinoflagellate, and is an ubiquitous form.

Primary production also shows a maximum at the front relative to either side (Fig. 7), however, the areal rate of primary production relative to the quantity of chlorophyll a in the euphotic zone is higher shoreward. It should be pointed out that incubations of this sort are subject to the vagaries of weather, and therefore the differences noted may

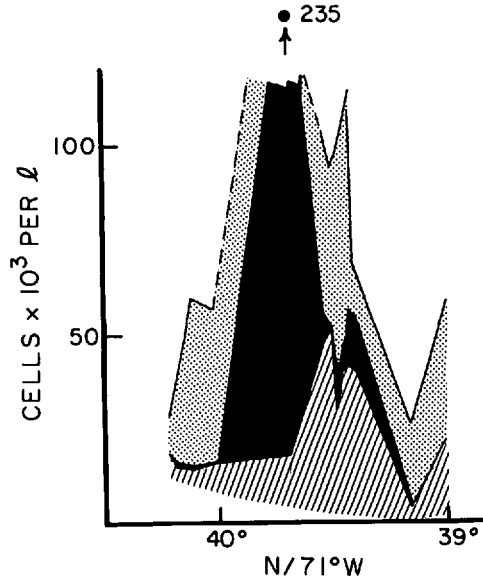


Figure 6. Major groups of phytoplankton, in terms of cell concentrations, found during the transects along 71W. Dotted area represents dinoflagellates, solid area is diatoms, and hatched area is flagellates. Diatom populations are mostly *Leptocylindrus danicus*, *Chaetoceros sp.*, and *Rhizosolenia faeroenese*. Dinoflagellates are almost entirely *Prorocentrum micans*.

represent local sun and cloud conditions and not the longer term mean. Nevertheless, these rates provide a benchmark useful to the analysis presented below. The integrated rates of primary production, from 200–400 mg C m⁻² d⁻¹, agree with the data (in summer) compiled by O'Reilly and Busch (1984) for this environment in the Middle Atlantic Bight.

4. Discussion

The biological distributions we have observed relative to the front are similar to that observed to HM83. The primary difference compared with the previous work is that we sampled for a time along the edge of a highly convoluted boundary caused by the influence of an anti-cyclonic eddy (Houghton *et al.*, 1986; Fig. 2). Reasons for the general enhancement of chlorophyll in the front is the subject of the remainder of the discussion.

It is difficult to see how loss processes, such as zooplankton grazing, could produce the distributions shown in Figures 3 and 4. Also, since zooplankton are generally variable over a larger spatial scale than phytoplankton growth (Steele, 1978; Mackas and Boyd, 1979), we must attribute the spatial variations in phytoplankton biomass at the front to the latter. The fact that maximum chlorophyll concentrations are located in the frontal zone (Fig. 3), a region we regard as a band of mixing between the shelf

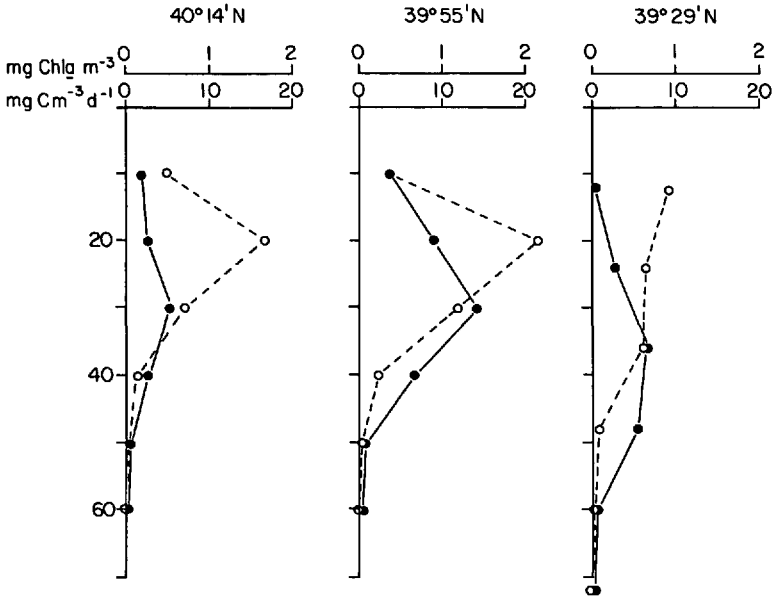


Figure 7. Depth distribution of photosynthetic carbon assimilation for the three experiments carried out during the cruise. The positions of these experiments are on the transect in Figure 2. Filled circles are chlorophyll values determined in the water samples, and open circles with dashed lines are carbon assimilation values. From left to right, areal production rates are 310, 410 and 204 mg C m⁻² d⁻¹.

and Slope Water, suggests that the frontal zone is also a region of enhanced phytoplankton growth. Alternatively, these populations may just be transported offshore. To examine these assertions we resort to a calculation based on a commonly-used growth and distribution model as a diagnostic for phytoplankton production across the region of the front.

Following the work, of for example, Riley *et al.* (1949), Kitchen *et al.* (1978), and Jamart *et al.* (1977) the equation for local change of phytoplankton can be written,

$$dP/dt = \kappa \nabla^2 P - u \nabla P + V_m NPL / (K_N + N) \quad (2)$$

Here, κ is the coefficient for eddy diffusivity for phytoplankton (P), and u is the advective term. For our purposes, the nutrient (N) will be represented by nitrate, therefore the phytoplankton concentration and production is in terms of nitrogen. V_m is the maximum rate of growth of the phytoplankton, K_N is nutrient concentration for which the growth rate is one half its maximal rate, and L is a function that adjusts the rates by the irradiance at a particular depth.

Since we are interested in the biological response of the phytoplankton in the frontal region, we neglect the physical terms in Eq. (2). That is, we allow the Lagrangian movement of the phytoplankton, (time-scale of 1–3 days) and we use the biological

term in a diagnostic way to describe the distribution of production across the front. Therefore, ignoring the diffusive and advective terms, we define a calculated production rate as,

$$dP/dt = p = V_m NPL / (K_N + N) \quad (3)$$

The units of p are $\mu\text{mol N m}^{-3} \text{d}^{-1}$. All the factors in this expression can be estimated from the data, with the exception of K_N and L which can be obtained or derived from the literature. Thus, we have set K_N to $0.3 \mu\text{M l}^{-1}$ nitrate, a value representative of summertime conditions (e.g., Tett *et al.*, 1986). We show below that the calculation is not sensitive to the choice of K_N .

Calculation of L required three steps. First, total daily (clear-sky) insolation values, E_{tot} , for the time of year and latitude of our measurements were obtained from the tables of Berger (1978). The total value for the photosynthetically active region of the irradiance spectrum, $E(0)$ was found by,

$$E(0) = 0.5 E_{\text{tot}}, \quad (4)$$

following Baker and Frouin (1987). Second, $E(z)$, the irradiance at depth z is determined using Eq. (1), repeated here,

$$E(z) = E(0) e^{-kz}, \quad (1)$$

where k is the attenuation coefficient. As described above, a piece-wise linear regression was used to obtain k as a function of latitude, and therefore station position (see Fig. 5). Third, L was determined as

$$L = [E(z)/E_{\text{max}}] \cdot \exp [1 - (E(z)/E_{\text{max}})]. \quad (5)$$

E_{max} was assigned the value of $177 \mu\text{Einsteins m}^{-1} \text{s}^{-1}$, following the experimental work of Malone and Neale (1981) for photosynthesis-irradiance relationships for phytoplankton in the region of this front.

Maximum growth rate was obtained from the productivity experiments (Fig. 8), the experimental determination of the carbon:chlorophyll ratio, and using the equation of Eppley (1972),

$$V_m = (1/t) \ln [\Theta + \Delta C \cdot \text{Chl}^{-1}] / \Theta \quad (6)$$

In this equation, Θ is the experimentally determined carbon:chlorophyll ratio, and $\Delta C/\text{Chl}$ is the maximum rate of primary production normalized to chlorophyll observed in the primary production experiments. With $\Theta = 133$, and the maximum $\Delta C/\text{Chl} = 40 \mu\text{g C} (\mu\text{g Chl})^{-1} \text{d}^{-1}$, we calculate V_m to be 0.3d^{-1} .

We have not considered ammonium as a nutrient, even though it could be considered a "new" nutrient in shelf water (Malone *et al.*, 1983) and therefore lead to a change in biomass distribution. The reason is that its concentration at the front is $<0.1 \mu\text{M l}^{-1}$,

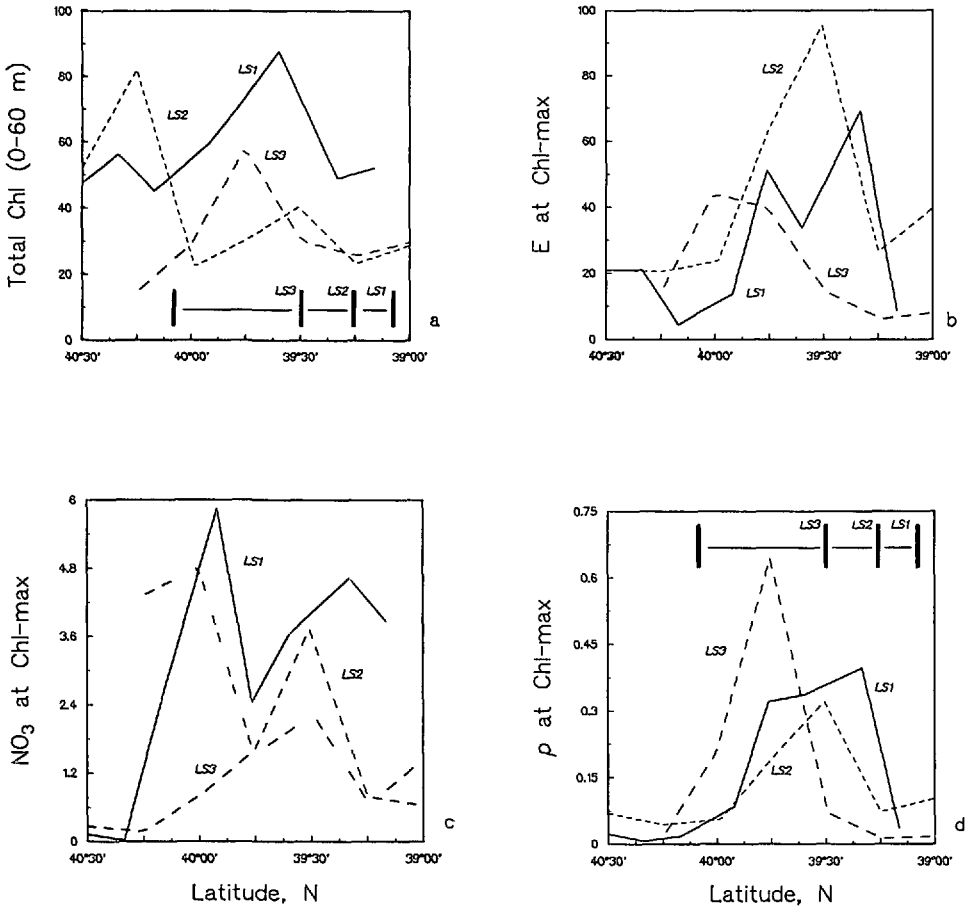


Figure 8. The variation of determinants to phytoplankton growth at the depth of the Chl-max along each of the three long sections of the cruise (LS1, LS2, LS3) across the front. The front, as we have defined it, is between 40°00'N and 39°25'N. (a) chlorophyll *a* (mg m^{-3}); (b) Irradiance ($\mu\text{Einstein m}^{-1} \text{s}^{-1}$); (c) NO_3 ; (d) production ($\mu\text{M N m}^{-3} \text{d}^{-1}$) as defined by Eq. (3) in the text. The horizontal line divided by bars shown in panels (a) and (d) indicate the width of the frontal zone (as defined in the text) during each of the three transects.

about an order of magnitude less than nitrate. It is unlikely to influence the rate of nitrate uptake (McCarthy *et al.*, 1975; Garside, 1981) and its potential to produce new biomass is small. Finally, we assume that the conversion of assimilated nitrate to chlorophyll is 1:1. That is 1 μmol nitrate becomes 1 μg chlorophyll. The evidence in support of this assumption is presented in Marra *et al.* (1990).

To visualize better the interplay of factors involved in p , we have plotted (Fig. 8) along latitude the other variables in the equation for the depth of the maximum chlorophyll (see Fig. 3). Experimentally, p will not be maximum at this depth, and this is borne out in our data (Fig. 7), however, this will not affect its spatial distribution. We

have chosen for illustration the three large-scale sections that took place on 19, 25 and 30 July, designated LS1, LS2, and LS3 (Fig. 8). The largest change in a factor influencing growth going across the front is irradiance in the water column (Fig. 8b), although nitrate shows effects as well (Fig. 8c). Nutrients are probably not as important since the bulk of the chlorophyll in the water column is within the nitrate gradient (and as we have stated, ammonium is $<0.1 \mu\text{M l}^{-1}$ throughout this region). All variables increase in the frontal zone. Total chlorophyll for LS2 is highest inshore of the front (Fig. 8a), perhaps arising from processes not revealed by our sampling. However, p is clearly at a maximum in the frontal zone for all three times during the cruise (Fig. 8d).

The foregoing evidence suggests the following scenario for the relative fertility of this region of the shelf-break front. As coastal water is drawn off the shelf, it moves upward along isopycnal surfaces. This upward inclination of the isopycnals brings nutrient-rich water shallower and into optically clearer water, allowing for a higher phytoplankton growth rate. This flow is roughly parallel to nutrient isopleths. Deep shelf water also has high levels ($>1 \mu\text{M}$) of ammonia. The absence of ammonium in the front suggests that it is rapidly utilized or else transformed through nitrification. Because it is ephemeral, we could not include it in our calculations, but this simplification does not affect the results shown in Figure 8.

A detailed description of the eddy presumed to have caused the offshore movement of coastal water is given by Houghton *et al.* (1986). This is inferred from a comparison of the T/S properties of the offshore boluses of water shown in Figure 4, and the deep shelf water. It appears that as this column of shelf water moved rapidly offshore, it was squeezed between the converging density surfaces which imparted anti-cyclonic vorticity (Fig. 2a). By this process, deep shelf water is upwelled into the euphotic zone at the frontal boundary with effective vertical velocities of the order $10\text{--}20 \text{ m d}^{-1}$. The combination of nutrient-rich water (which is in an otherwise turbid environment), and clear water (which is in an otherwise nutrient-poor environment) are the ingredients for high phytoplankton growth at the summertime baroclinic front. Thus we have a classic case where the mixing of different water types has a favorable effect on the plankton populations. Our calculation treats only the biological result of this frontal circulation, not the circulation itself. Sustained phytoplankton production at the front would rely on other processes to bring nutrients into the surface layer.

The small-scale circulation inferred from various theoretical studies of frontal dynamics does not produce an upwelling pattern or biological distribution that is consistent with this scenario. For instance, an Ekman frictional layer along the frontal interface (Garrett and Loder, 1981), or geostrophic adjustment following a wind- or buoyancy-induced mixing event (Ou, 1984), result in sinking water on the Slope Water side of the front. Csanady (1984) and Csanady and Hamilton (1988) suggest a broad region of upwelling between the shelf break front and the Gulf Stream in response to wind-forcing. Estimated vertical velocities, at 0.5 m d^{-1} , are of the right order, but the

upwelling is postulated to extend far out into the Slope Water region and is not confined to the front as are the high chlorophyll concentrations here. Second, the magnitude of the upwelling velocity is appropriate for the winter and spring seasons with higher wind speeds, and certainly not the summer when the wind stress is an order of magnitude smaller.

The relationship of the region of high phytoplankton growth to the front is similar to that observed in spring (Marra *et al.*, 1982). Phytoplankton growth and biomass are greatest just shoreward of, or at, the baroclinic boundary. Water column irradiance is the important controlling factor for production for both time periods. It is possible that these inferences can be applied to other frontal regions (e.g., Fournier *et al.*, 1977) where sharp differences occur in water mass characteristics.

In the Middle Atlantic Bight, frontal eddies appear to be common events. Garvine *et al.* (1988) describe in detail an encounter with a pair of cyclonic eddies. As we have seen, a hydrographic section through an eddy often shows what appears to be a detached bolus of shelf water. Therefore, the boluses of shelf water in the Slope Water region that have been frequently detected in the historical data record (Cresswell, 1967; Wright, 1976) may actually indicate the occurrence of eddy events.

The mechanism that drives the eddy-jets of shelf water offshore is still obscure. Presumably it is related to the changing hydrographic conditions along the continental margin in the summer, although similar small-scale frontal eddies are observed in satellite (AVHRR) imagery during other times of the year. During the year-long SEEP-I thermistor array on the New England Shelf (Houghton *et al.*, 1988) when warm-core rings were absent, offshore boluses of shelf water were observed only during the summer and early fall. Baroclinic instability is a suspected cause of these features, and although attempts to model the process are encouraging (Gawarkiewicz, personal communication), the efficacy of this mechanism has yet to be demonstrated and remains an important problem in frontal dynamics.

These results give a new dimension to the potential for off-shelf transport of shelf populations, postulated by Walsh (1983, 1988) and inferred for wintertime populations for the southeastern United States continental shelf (Yoder and Ishimaru, 1989). While the significance of this phenomenon can be debated (Falkowski *et al.*, 1988), it appears that population growth can occur in a region (the summertime front) overlaying the continental slope. This may resolve some of the differences between Walsh (1988) and his critics (Rowe *et al.*, 1986; Falkowski *et al.*, 1988). In other words, rather than biomass, production (or a production "capacity") is being transported off the shelf. Since it is supported by nitrate, it can be termed new production. As such, the significance of the phenomenon of off-shelf transport of phytoplankton may be better understood through the dynamics of nutrient transport rather than chlorophyll.

We can calculate the significance of this nutrient transport. Given the volume of the shelf water in the eddy (Figs. 3, 4; see also Figure 6 of Houghton *et al.*, 1986; 30 m thick by 2×10^9 m² in area) and an average nitrate concentration of 6 mM m⁻³, means

that this event was responsible for exporting 5.1×10^3 t N to the Slope Water. The frequency of such events are unknown, but we can evaluate, roughly, this event with respect to production on the shelf. The range of 'new' (nitrate supported) production in the shelf area shoreward of this region of the front ranges 1–7 mmol N m⁻² d⁻¹ (Harrison *et al.*, 1983), or $9\text{--}66 \times 10^3$ t N for a 75 km × 75 km area for 120 d. Therefore it would require 2–10 of these frontal events to equal that rate of nitrate-supported production in summer.

Acknowledgments. We thank D. Boardman, J. Garside, K. Heinemann, B. Huber, M. Maccio and G. Tilton for assistance at sea. D. Schneider provided excellent assistance with data reduction. This research was supported by the National Science Foundation under grants OCE-82-09799 (JM and RWH) and OCE-82-14776 (CG), and by Office of Naval Research Contract N-00014-84-C0132 (JM). This is LDGO contribution no. 4713 and Bigelow Laboratory for Ocean Sciences contribution no. 90015.

REFERENCES

- Baker, K. S. and R. Frouin. 1987. Relation between photosynthetically active available radiation and total insolation at the ocean surface under clear skies. *Limnol. Oceanogr.*, **32**, 1370–1377.
- Berger, A. L. 1978. A simple algorithm to compute long term variations of daily or monthly insolation, *Contr. No. 18*, in Institut d'astronomie et de geophysique. Georges Lemaitre, U. Catholique, Louvain, Belgium.
- Cresswell, G. H. 1967. Quasi-synoptic monthly hydrography of the region between coastal and slope water south of Cape Cod, Mass. W.H.O.I. Ref. No. 67-35 (unpublished manuscript).
- Csanady, G. T. 1984. The influence of wind stress and river runoff on a shelf-sea front. *J. Phys. Oceanogr.*, **14**, 1383–1392.
- Csanady, G. T. and P. Hamilton. 1988. Circulation of slope water. *Cont. Shelf Res.*, **8**, 565–623.
- Eppley, R. W. 1972. Temperature and phytoplankton growth in the sea. *Fish. Bull.*, **70**, 1063–1086.
- Falkowski, P. G., C. N. Flagg, G. T. Rowe, S. L. Smith, T. E. Whitedge and C. D. Wirick. 1988. The fate of the spring phytoplankton bloom: export or oxidation. *Cont. Shelf Res.*, **8**, 457–484.
- Fournier, R. O., J. Marra, R. Bohrer and M. Van Det. 1977. Plankton dynamics and nutrient enrichment of the Scotian Shelf. *J. Fish Res. Board Can.*, **34**, 1004–1018.
- Garrett, C. J. R. and J. W. Loder. 1981. Dynamical aspects of shallow sea fronts. *Phil. Trans R. Soc. Lond.*, **A 302**, 563–582.
- Garside, C. 1981. Nitrate and ammonium uptake in the apex of the New York Bight. *Limnol. Oceanogr.*, **26**, 731–739.
- Garvine, R. H., K.-C. Wong, G. G. Gawarkiewicz, R. K. McCarthy, R. W. Houghton and F. Aikman III. 1988. The morphology of shelf-break eddies. *J. Geophys. Res.*, **93**, 15,593–15,607.
- Gordon, A. and F. Aikman III. 1981. Salinity maximum in the pycnocline of the Middle Atlantic Bight. *Limnol. Oceanogr.*, **26**, 123–130.
- Harrison, W. G., D. Douglas, P. G. Falkowski, G. Rowe and J. Vidal. 1983. Summer nutrient dynamics of the Middle Atlantic Bight: Nitrogen uptake and regeneration. *J. Plank Res.*, **5**, 539–556.
- Holligan, P. M. and S. B. Groom. 1986. Phytoplankton distributions along the shelf break. *Proc. Royal Soc. Edinburgh*, **88B**, 239–263.
- Holm-Hansen, O., C. J. Lorenzen, R. W. Holmes and J. D. H. Strickland. 1965. Fluorometric determination of chlorophyll. *J. Conseil.*, **30**, 3–15.

- Horrocks, D. L. 1977. The H Number concept. Beckman Instruments Technical Report 1095 NUC-77-1T.
- Houghton, R. W., F. Aikman III and H. W. Ou. 1988. Shelf/slope frontal structure and cross-shelf exchange on the New England shelf. *Cont. Shelf Res.*, **8**, 687–710.
- Houghton, R. W. and J. Marra. 1983. Physical/biological structure and exchange across the thermohaline shelf/slope front in the New York Bight. *J. Geophys. Res.*, **88**, 4467–4481.
- Houghton, R. W., D. B. Olson and P. J. Celone. 1986. Observation of an anticyclonic eddy near the continental shelf break south of New England. *J. Phys. Oceanogr.*, **16**, 60–71.
- Houghton, R. W., R. Schlitz, R. C. Beardsley, B. Butman and J. L. Chamberlin. 1982. The Middle Atlantic Bight Cold Pool: Evolution of the Temperature Structure During Summer 1979. *J. Phys. Oceanogr.*, **12**, 1019–1029.
- Jamart, B. M., D. F. Winter, K. Banse, G. C. Anderson and R. K. Lam. 1977. A theoretical study of phytoplankton growth and nutrient distribution in the Pacific Ocean off the northwestern U.S. Coast. *Deep-Sea Res.*, **24**, 753–773.
- Kinder, T. H., G. L. Hunt, Jr., D. Schneider and J. D. Schumacher. 1983. Correlations between seabirds and oceanic fronts around the Pribilof Islands, Alaska. *Est., Coastal Shelf Sci.*, **16**, 309–319.
- Kitchen, J. C., J. R. V. Zaneveld and H. Pak. 1978. The vertical structure and size distributions of suspended particles off Oregon during the upwelling season. *Deep-Sea Res.*, **25**, 453–468.
- Mackas, D. L. and C. M. Boyd. 1979. Spectral analysis of zooplankton spatial heterogeneity. *Science*, **204**, 62–64.
- Malone, T. C. 1977. Plankton systematics and distribution, MESA New York Bight Atlas Monogr. 13, New York Sea Grant Institute, Albany, NY, 45 pp.
- Malone, T. C., T. S. Hopkins, P. G. Falkowski and T. E. Whitledge. 1983. Production and transport of phytoplankton biomass over the continental shelf of the New York Bight. *Cont. Shelf Res.*, **1**, 305–337.
- Malone, T. C. and P. J. Neale. 1981. Parameters of light-dependent photosynthesis for phytoplankton size fractions in temperate estuarine and coastal environments. *Mar. Biol.*, **61**, 289–297.
- Marra, J., R. R. Bidigare and T. Dickey. 1990. Nutrients and mixing, chlorophyll and phytoplankton growth. *Deep-Sea Res.*, **37**, 129–143.
- Marra, J., R. W. Houghton, D. C. Boardman and P. J. Neale. 1982. Variability in surface chlorophyll *a* at a shelf-break front. *J. Mar. Res.*, **40**, 575–591.
- McCarthy, J. J., W. R. Taylor and J. Taft. 1975. The dynamics of nitrogen and phosphorus cycling in the open waters of the Chesapeake Bay, *in* Marine Chemistry in the Coastal Environment, T. C. Church, ed., Amer. Chem. Soc. Symp. No. 18. Wash., DC, 664–681.
- O'Reilly, J. E. and D. A. Busch. 1984. Phytoplankton primary production on the Northwestern Atlantic shelf. *Rapp. P.-v. Reun. Cons. int. Explor. Mer.*, **183**, 255–268.
- Ou, H. W. 1984. Geostrophic adjustment: a mechanism for frontogenesis. *J. Phys. Oceanogr.*, **14**, 994–1000.
- Pingree, R. D. 1978. Cyclonic eddies and cross-frontal mixing. *J. Mar. Biol. Assoc. U.K.*, **59**, 689–698.
- Pingree, R. D., P. R. Pugh, P. M. Holligan and G. R. Forster. 1975. Summer phytoplankton blooms and red tides along tidal fronts in the approaches to the English Channel. *Nature*, **258**, 672–677.
- Riley, G. A., H. Stommel and D. F. Bumpus. 1949. Quantitative ecology of the plankton of the Western North Atlantic. *Bull. of the Bingham Oceanogr. Coll., Yale University*, **12**, 1–169.

- Rowe, G. T., S. Smith, P. Falkowski, T. Whitedge, R. Theroux, W. Phoel and H. Ducklow. 1986. Do continental shelves export organic matter? *Nature*, 324, 559–561..
- Steele, J. H. 1978. Some comments on plankton patches. *in* Spatial Pattern in Plankton Communities, J. H. Steele, ed., Plenum, NY, 1–20.
- Tett, P., A. Edwards and K. Jones. 1986. A model for the growth of shelf-sea phytoplankton in summer. *Est. Coastal Shelf Sci.*, 23, 641–672.
- Walsh, J. J. 1983. Death in the sea: enigmatic phytoplankton losses. *Prog. Oceanogr.*, 12, 1–86.
- 1988. *On the Nature of Continental Shelves*. Academic Press, New York, 520 pp.
- Whitedge, T. E., S. C. Malloy, C. J. Patton and C. D. Wirick. 1981. Automated nutrient analyses in seawater. Dept. Energy and Environment, BNL 51398, 216 pp.
- Wright, W. R. 1976. The limits of shelf water south of Cape Cod, 1941–1972. *J. Mar. Res.*, 34, 1–14.
- Yoder, J. A. and T. Ishimaru. 1989. Phytoplankton advection off the southeastern United States continental shelf. *Cont. Shelf Res.*, 9, 547–553.

